Biomass Conversion and Biorefinery (2024) 14:20385–20396
https://doi.org/10.1007/s13399-023-04225-6

ORIGINAL ARTICLE

Preparation and characterization of hydrochars and CO_2-activated hydrochars from date and olive stones

Ahmed Bourafa[1,2] · Emna Berrich[2] · Meriem Belhachemi[1] · Salah Jellali[3] · Mejdi Jeguirim[4]

Received: 19 January 2023 / Revised: 12 April 2023 / Accepted: 14 April 2023 / Published online: 28 April 2023

Abstract

Agriculture and food processing waste valorization is a sustainable process to protect the environment and to produce high added–value products. In this context, this study focuses on the conversion of two abundant agrifood residues largely available in Algeria, namely date pits and olive stones into carbonaceous materials. These biomasses were hydrothermally carbonized at 220 °C for various residence times ranging between 10 and 48 h. Then, the derived hydrochars were activated at 750 °C for 1 and 3 h under a carbon dioxide (CO_2) atmosphere. Several techniques were used to characterize the obtained carbonaceous materials including gas adsorption, scanning electron microscopy (SEM), Fourier transform infrared (FTIR), Raman, and X-ray diffraction spectroscopy. Results showed that the obtained hydrochars present high mass yields, important amounts of oxygen groups, relatively low porosities, and low specific surface area (less than 24 m^2/g for all hydrochars). However, the derived activated carbons (after 1 h of CO_2 activation) show an increase of specific surface areas to 449 and 562 m^2/g for date pits and olive stones, respectively. Moreover, the hydrochar activation process leads also to the development of both narrow and large micropores. The increase in the residence time favors the formation of carbon microspheres and increases the microcrystallites (*aromatic rings*). This spherical structure development is significantly promoted after the activation process. Therefore, the produced activated carbons have interesting textural, structural, and chemical properties indicating their potential for pollutants removal from aqueous and gaseous effluents.

Keywords Hydrothermal carbonization · Hydrochar · Spherical activated carbon · CO_2 activation · Date and olive stones

1 Introduction

According to the Directive 2009/28/EC [1], biomass is designated as biodegradable products, wastes, and residues of biological origin from agriculture (plant and animal substances), forestry, and related industries, including fishing and aquaculture, as well as the biodegradable fraction of industrial and municipal wastes. Biomass is also considered a clean and abundant renewable resource that could play several roles in the sustainable development. In particular, biomass can be used for energy production [2], carbon sequestration, and also as a major component in the production of carbonaceous materials and biofuels [3, 4]. The use of biomass feedstocks to produce carbonaceous materials such as biochars and hydrochars is well desired since it could provide reliable solutions for solid waste management, lower the cost of raw materials, and allow the finished product quality to be adjusted for various uses [5].

Algeria has many agro-food factories and farms generating huge amounts of unexploited agrifood wastes. The total amount of agricultural wastes generated by the country was estimated to be around 13.6 million tons per year in 2019 [6]. Basically, biomass is used as animal food or dumped in nature in a hazardous manner causing severe damage to the environment. According to recent statistics available from the Algerian press service and the Directorate of Agricultural Services (DAS), Algeria produced about 1.2 million

✉ Meriem Belhachemi
bel_meriem@yahoo.fr

1 Laboratory of Chemistry and Environmental Science, University Tahri Mohamed Bechar, 08000 Béchar, Algeria

2 UMR CNRS 6144, DSEE, GEPEA, Nantes University, IMT Atlantique, 4 Rue Alfred, Kastler, BP20722 44307 Nantes Cedex 03, France

3 Center for Environmental Studies and Research, Sultan Qaboos University, Al-Khoudh 123, Muscat, Oman

4 The Institute of Materials Science of Mulhouse (IS2M), UMR 7361, University of Haute Alsace, University of Strasbourg, CNRS, 68100 Mulhouse, France

tons of dates and more than 1.0 million tons of olives in 2019 [7].

The biomass conversion into useful products or energy can be performed by different techniques such as hydrothermal carbonization, dry torrefaction, and pyrolysis. Hydrothermal carbonization (HTC) is defined as a thermochemical conversion process of wet precursors into added-value products such as hydrochars and biofuels [3, 5, 8]. The HTC method is an exothermic process employing subcritical water (hot water under pressure) to transform humid biomass into carbonaceous materials produced by lowering both the precursor oxygen and hydrogen contents (as measured by the molecular O/C and H/C percentages) through dehydration and decarboxylation reactions [3]. The production temperature is generally between 170 and 280 °C, and the pressure is autogenously (2–5 MPa). Typically, the reaction pressure is uncontrolled and autogenic with a saturation vapor pressure corresponding to the reaction temperature [9, 10]. When compared with pyrolysis, the HTC process has numerous benefits such as relatively low operating temperature during carbonization, the ability to use biomass having high moisture contents, and the development of carbonaceous materials with specific developed surface morphology (for example, a hollow spherical structure) and chemistry (richness in oxygen functionalities such as hydroxyl and carboxyl groups). These properties improve hydrochar chemical reactivity and promote their use in various applications such as adsorption and catalysis [10–12]. Hydrochar prepared from biomass can be used as precursors in many fields including energy production, soil amendment, and gas storage [10, 13–15]. Moreover, hydrochars have been recently considered efficient adsorbents. Generally, a carbonaceous adsorbent can be defined as a material mainly composed of carbon with appropriate porosity (high surface area and micropore volume) and chemical surface proprieties improving its ability to retain molecules onto its surface [10]. Among various carbonaceous adosrbents, activated carbons (ACs) have been distinguished for their large applications. Therefore, new preparation methods are used in order to get the most-efficient physical forms and structures. ACs are usually obtained by physical or chemical activation [16]. Physical activation is a technique used to improve the porous properties of carbonaceous materials. The thermal (physical) activation is usually achieved by using CO_2, steam, or a mixture of these oxidizing gases [14] at quite high temperatures, often between 700 and 900 °C.

In this study, the production of hydrochars from abundant wastes (date pits and olive stones) and their corresponding activated carbons is reported. The preparation of ACs from hydrochars may be a saving energy method compared to the pyrolysis process since the used temperature treatment is usually lower for the case of HTC. The use of hydrochars as precursors for producing ACs has shown interesting results in porosity and chemical surface properties development [17, 18]. In the available literature, there is no investigation on the characterization of ACs produced by CO_2 activation of hydrochars derived from date pits and olive stones. For this purpose, textural and chemical structural proprieties of hydrochars and activated hydrochars are investigated in this present study. Moreover, the development of the AC porosities is assessed as a function of the activation degree.

2 Materials and methods

2.1 Feedstock preparation protocol

Date pits and olive stones were used for the production of hydrochars. Date pits were obtained from a date paste production plant in Biskra Province, in the southeast of Algeria. The olive pomace wastes were collected from an olive oil mill in Mila Province (Northeast of Algeria). These biomasses were washed with water and then dried in an oven at 105 °C for 12 h and then grounded and sieved to retain the fractions between 0.5–1 mm and 1–2 mm, respectively.

2.2 Experimental procedure

2.2.1 Hydrothermal carbonization (HTC)

The HTC experiments were achieved in an autoclave of type Top Industrie (Vaux le Penil, France) with a capacity of 250 mL (Fig. 1). It consists of two parts: an internal, removable, and inert part made of PTFE (polytetrauoroethylene) in which the reagents are introduced, and an external part made of stainless steel allowing to keep the system tight during the whole experiment.

In this work, around 10 g of biomass (fruit stones) and 30 g of water (corresponding to a solid/liquid ratio of 1:3) are introduced into the internal part of the PTFE autoclave.

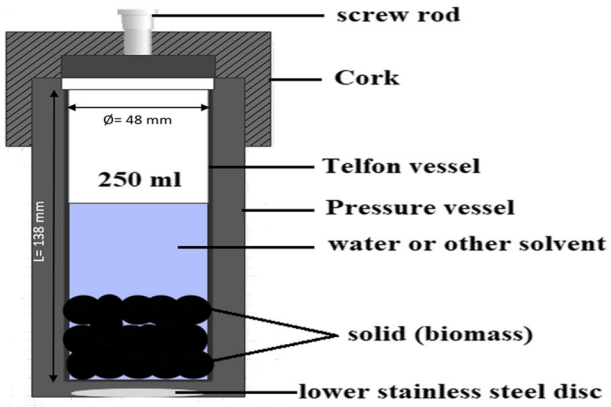

Fig. 1 Schematic diagram of the used autoclave

The system (autoclave with reagents) is then placed in an oven at temperatures of 220 °C for a given time "t" + 30 min. This 30-min duration is considered equivalent to the rise in temperature in the autoclave. During this work, the HTC was fixed to 220 °C. This parameter value permits to obtain hydrochars with interesting physico-chemical properties [10, 19]. The effect of the residence times was assessed at 10, 24, and 48 h. At the end of this HTC process, the autoclave was kept to be naturally cooled to ambient temperature. The solid phase was then separated from the liquid one by simple filtration. Then, this solid residue was rinsed four times with distilled water in order to completely remove tar and bio-oil and afterward dried at 105 °C in the oven for 12 h. The synthesized hydrochars were denoted "P–t," where "P" represents the precursor (DS, date stones; OS, olive stones), and "t" is the residence time of carbonization. For example, DS-24 represents the hydrochar sample issued from date stones prepared by HTC at a temperature of 220 °C and a residence time of 24 h.

2.2.2 Synthesis of activated carbons

This step concerns the synthesis of ACs from the prepared hydrochars using physical activation with CO_2. These spherical activated carbons were prepared by using N_2 and CO_2 (Fig. 2). During this research work, the temperature and heating rate of the activation process were fixed to 750 °C and 10 °C/min, respectively. These optimal values were deduced from previous investigations [14, 20, 21]. Practically, the hydrochars issued from date pits or olive stones were heated in a horizontal tubular furnace for a constant gradient of 10° C/min and under an inert gas of N_2 (40 mL/min). When the activation temperature (750 °C) was attained, the N_2 gas was switched to CO_2 and the activation continued for a chosen time (1 or 3 h). Then, the activated carbon was cooled under N_2 to room temperature.

The obtained spherical activated carbons were labelled O (olive) or D (date) S (stones); a–b, which represent the hydrothermal carbonization time and the activation time, respectively. For example, the activated carbon OS-24–1 is prepared from the hydrochar OS-24 and activated for 1 h under CO_2.

The burnoff values of the synthetized ACs (BO (%)) were calculated according to the following expression:

$$BO = \frac{Wt0 - Wt}{Wt0} \cdot 100$$

where W_{t0} and W_t are the initial mass of the hydrochar and the final mass of the corresponding activated carbon, respectively.

2.3 Characterization of hydrochars and activated carbons

2.3.1 Elemental composition analysis

The elemental composition in terms of moisture (wt. (%)), carbon (C), hydrogen (H), nitrogen (N), and sulfur (S) of the raw samples, hydrochars, and the activated carbons was determined by using an analyzer "Flash EA1112, THERMO FINNIGAN."

2.3.2 Textural and surface morphology characterizations

The textural properties of the synthetized hydrochars and ACs were carried out by using a BET apparatus test "Micromeritics Smart VacPrep." This technique is applied to calculate the specific surface area and pore volumes of hydrochars and activated carbons from the quantity of nitrogen (N_2) and carbon dioxide (CO_2) adsorbed at boiling temperatures of − 196.15 °C and 0 °C, respectively. The specific surface area N_2 (S_{BET}) was calculated using the BET equation. The narrow or ultra micropore (< 0.7 nm) volume "$V(CO_2)$" and the wide or super micropore (0.7–2 nm) volume "$V_{mi}(N_2)$" were determined from CO_2 and N_2 adsorption isotherms using the Dubinin-Radushkevich equation.

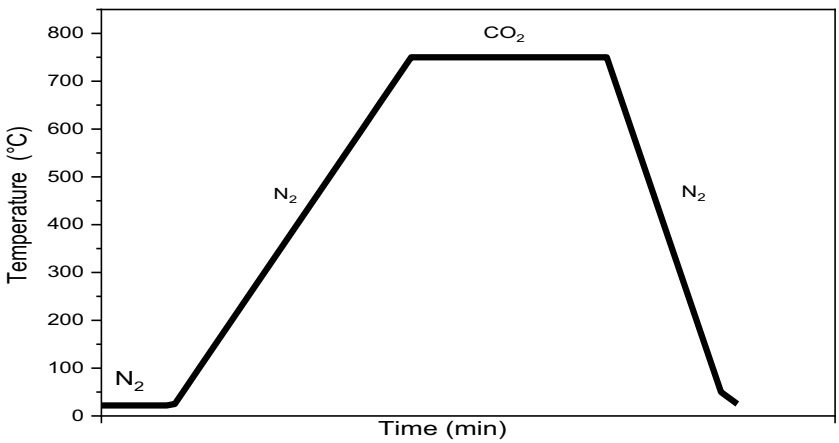

Fig. 2 Used hydrochar activation process

The total volume (V_T) was deduced at relative pressure equal to 0.95 and the mesopore volume (V_{me}) was calculated from the difference between the total and micropore volumes.

Moreover, scanning electron microscopy (SEM) analyses were used to determine the surface morphology of hydrochars and activated carbons. The images were obtained through JEOL JSM 5800LV apparatus.

2.3.3 Surface chemistry

Fourier transform infrared (FTIR) technique was used to identify the different chemical groups present in the surface of the synthetized carbonaceous materials. Hence, hydrochars and activated carbons were ground to a fine diameter and analyzed. Measurements have been made for 32 s in the range of 400 to 4000 cm^{-1} using the infrared spectrometer Bruker (VERTEX 70 Fourier).

2.3.4 Structure characterization

In order to study the structure of the prepared hydrochars and activated carbons, Raman and XRD analyses were carried out. Raman analysis was performed on a Renishaw InVia spectrometer with a microscopic setup, using an exciter line of the Argon laser with wavelength $\lambda = 514.5$ nm. The used laser is of 2 mW power and is focused on the sample with a 20 × and 50 × objective having a depth of 8 mm, with a scan of 100 to 4000 cm^{-1}. In addition to Raman, an X-ray diffraction (XRD) apparatus (SEIFERT Analytical X-ray M2 VIE) was used to identify the crystalline phases present in the prepared materials. Analyses were carried out using a Cu-K radiation source operating at a voltage of 40 kV. The diffraction angle (2Θ) was changed from 2.5 to 10° for the activated carbons and from 10 to 80° for the hydrochars [22].

3 Results and discussion

3.1 Elemental analysis

Table 1 shows the elemental analysis of the two raw materials (olive stones and date pits), and the synthetized hydrochars and activated carbons. For all hydrochars, as expected, when increasing the residence time, the carbon contents increase, while the fractions of oxygen decrease, and the contents of hydrogen remain almost constants. The nitrogen contents slightly increase for hydrochars issued from date pits. However, the percent weight of sulfur is below the detection limit.

The atomic ratios were determined and evaluated in a Van Krevelen diagram, to accurately describe how raw material hydrochars and activated carbon atomic compositions change. The change in carbon contents from the biomass to hydrochar products is more pronounced for date pits than olive stones (Fig. 3). This behavior can be explained by the nature composition of the biomass samples. The evolution of the O/C and H/C ratios shows the degree of deoxygenation of the biomass, either by decarboxylation or by dehydration. These processes allow the elimination of oxygen and hydrogen in the form of CO_2 and H_2O, which results in less smoke being generated during the HTC [23]. The Van-Krevelen diagram (Fig. 3) exhibits that the HTC treatment decreases the O/C and H/C atomic ratios of date and olive stones. The evolution of the O/C and H/C atomic ratios of the hydrochars indicates that the HTC of the date and olive stones occurred essentially via dehydration reactions by removing oxygen in the form of water. The obtained results are in agreement with the literature suggesting that biomass loses hydroxyl, carboxyl, and carbonyl groups, which lead to the cleavage of aliphatic side chains that increases the aromaticity of the carbon materials [24, 25]. The activation of hydrochars leads

Table 1 Elemental analysis of raw materials, hydrochars, and activated carbons

Désignation	*%N*	*%C*	*%H*	*%O*[a]	*%S*	*H/C*	*O/C*	*%ash*
OS-raw	2.32	47.89	5.64	43.24	< L.D	1.41	0.68	0.91
OS-10	0.21	64.17	4.79	30.62	< L.D	0.89	0.36	0.26
OS-24	< LQ	67.08	4.86	27.80	< L.D	0.87	0.31	0.21
OS-48	< LQ	68.83	4.63	26.34	< L.D	0.81	0.29	0.20
OS-24.1	< LQ	88.52	0.90	10.58	< L.D	0.12	0.09	LQ
DS-raw	0.81	45.61	6.53	47.05	< L.D	1.72	0.77	0.96
DS-10	1.58	69.28	6.08	22.46	< L.D	1.05	0.24	0.60
DS-24	1.58	70.07	6.03	21.98	< L.D	1.03	0.23	0.34
DS-48	1.71	71.54	5.78	20.86	< L.D	0.97	0.22	0.11
DS-24.1	1.92	81.73	0.71	15.64	< L.D	0.10	0.14	LQ

([a]by difference: O = 100 − (C + H + N + ash); < *LD*, below detection limit (LD < 0.06% on CHNS-O); < *LQ*, below the limit of quantification (LQ < 0.2% on CHNS-O)

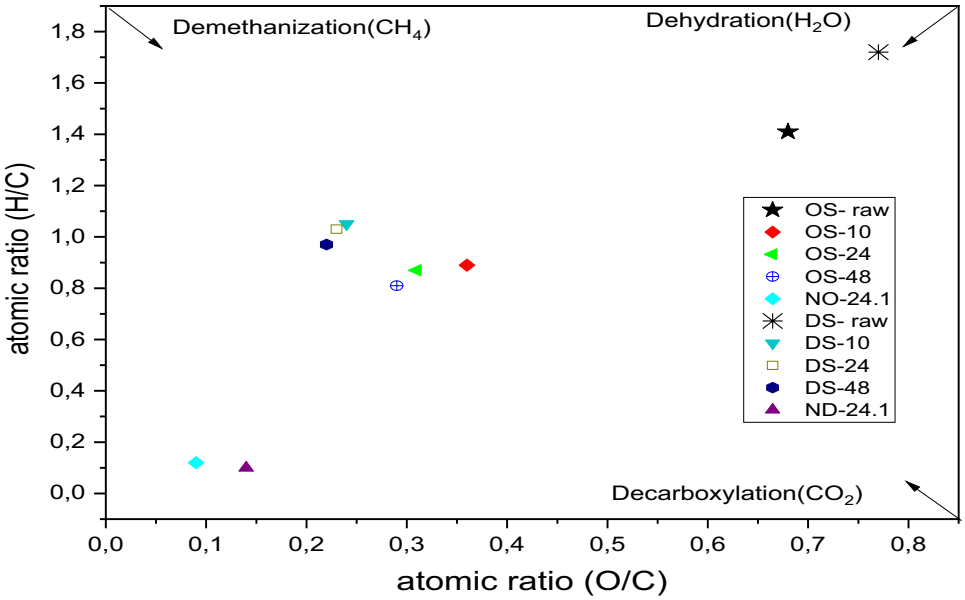

Fig. 3 Van Krevelen diagram for the biomasses, synthetized hydrochars, and activated hydrochars

to an additional increase in carbon contents and a reduction of oxygen and hydrogen quantities [26].

3.2 Textural and surface morphology proprieties

3.2.1 Textural properties

Figure 4a–b exhibits the N_2 adsorption–desorption isotherms of the hydrochars derived from date and olive stones as well as the spherical activated carbons produced by CO_2 activation. Additionally, the related textural parameters obtained from the N_2 and CO_2 adsorption are reported in Table 2. Figure 4a shows a poor adsorption behavior at low relative pressures and an important adsorption increase at $P/P_0 > 0.9$. All the samples analyzed have low BET surface areas between 17 and 22 $m^2.g^{-1}$ for the hydrochars issued from olive stones, and between 17 and 24 $m^2.g^{-1}$ for the date stones. Moreover, increasing the time of carbonization, the narrow micropore (V_{CO2}), and the total pore volume (V_T) slightly increase. The pore

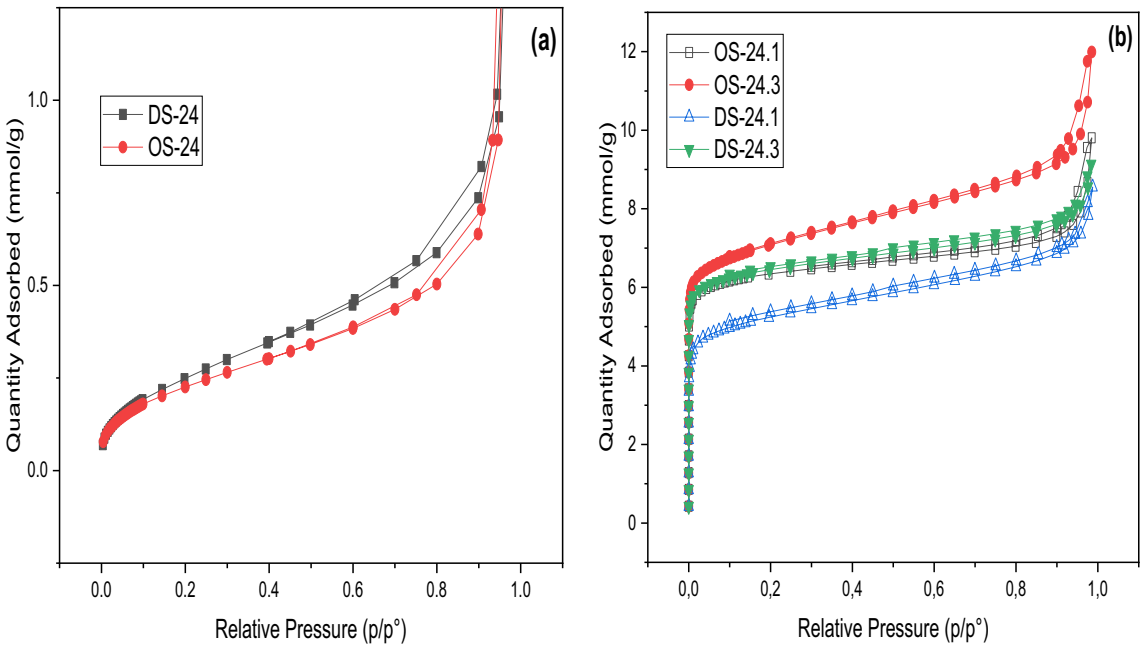

Fig. 4 Nitrogen adsorption–desorption isotherms at − 196 °C for **a** hydrochars and **b** activated carbons

Table 2 BET surface area and micro and mesopore volumes of hydrochars and activated carbons issued from the date and olive stones

Precursor	Sample	Yield	Burn off (%)	S_{BET} ($m^2.g^{-1}$)	V_T ($cm^3.g^{-1}$)	Vmi (N_2) ($cm^3.g^{-1}$)	Vme ($cm^3.g^{-1}$)	V(CO_2) ($cm^3.g^{-1}$)
HC-olive stones	OS-10	59.3	/	17.0	0.025	0.006	0.019	0.035
	OS-24	52.2	/	18.8	0.024	0.006	0.018	0.041
	OS-48	50.9	/	22.2	0.033	0.006	0.027	0.050
HC-date stones	DS-10	48.9	/	17.6	0.022	0.005	0.017	0.047
	DS-24	47.5	/	20.8	0.028	0.007	0.021	0.052
	DS-48	43.5	/	24.0	0.030	0.008	0.022	0.052
AC-OS	OS-24.1	/	49.0	562.0	0.261	0.214	0.047	0.161
	OS-24.3	/	51.3	606.0	0.325	0.229	0.096	0.169
AC-DS	DS-24.1	/	55.0	448.8	0.243	0.170	0.073	0.156
	DS-24.3	/	57.1	565.5	0.270	0.215	0.055	0.167

volume (V_T) values are low since they are in the range of 0.025–0.033cm^3/g and 0.022–0.030 cm^3/g for the hydrochars generated from olive stones and date stones, respectively. These results are coherent with those reported in previous works [27–29]. This low porosity of hydrochars could be due to pore-clogging caused by volatile materials that did not reach the liquid phase after the HTC treatment [29].

On the other hand, activated carbons obtained from the hydrochars show high N_2 adsorption (Fig. 4b). The isotherms exhibit the same shape which are characteristics of microporous materials, with the presence of mesopores for the sample OS-24–3 (presence of the hysteresis loop). The OS-24–3 shows the highest mesoporous volume (Table 2).

After the hydrochar activation, the surface area and pore volume of the AC significantly increase with the activation time. Indeed, by increasing the activation time from 1 to 3 h, the burnoff slightly increases about 2%; while important development of porosity is achieved. The BET surface areas become larger (448.8–565.5 $m^2.g^{-1}$) for date stones and (562.0–606.0 $m^2.g^{-1}$) for olive stones. These results are larger than the BET surface area of ACs issued from olive stones, sunflower stem, and walnut shell hydrochars activated with CO_2 (850 °C during 30 min). From Table 2, it can also be observed that the narrow micropore and super micropore volumes (V (CO_2) and V_{mi} (N_2)) increase with the burnoff (activation degree). Thus, the CO_2 activation of hydrochars develops micro- and meso-pores. These results are consistent with the role of this activating agent that usually creates narrow micropores and broadens the existing pores in the material [4, 14]. Such results also indicate that the CO_2 activation of chars or hydrochars issued from biomass acts in the same way when producing activated carbons. Whereas, it is important to note that hydrochars are more reactive than conventional chars. The hydrochar AC reached 50% of burnoff rapidly compared to biochar AC using the same precursor and activation conditions [14].

3.2.2 Surface morphology

The resulting hydrochars of the two precursors are brown with some black particles, which corresponds to partially carbonized materials. Analysis using microscopy techniques (Figs. 5 and 6) showed important changes in the raw material. Indeed, for the hydrochars obtained from date stones, the SEM images show the appearance of spheres from a carbonization residence time of 10 h. The development of these spherical carbon continues with the increase of the carbonization time. While for the synthetized hydrochar at a duration of 48 h, a bursting of these spheres is clearly noticed. In general, the particles keep the cellular structure of the biomass, though they are microspheres on the surface, which are probably produced from the transformation of the cellulosic fraction. Similar behavior was noted by Kang Set al. who revealed that microspheres were generated by the polymerization reaction in a solution of the hydrolyzed cellulose, such as glucose [30].

These microspheres have different diameters (Figs. 5c and 6c.), which may mainly represent the transformation of cellulose and lignin hydrolyzed particles. On the other hand, most of the spheres are grouped together. This indicates that the conditions of the hydrothermal carbonization of the biomasses are not optimal. At this stage, the formed hydrochar spheres have not developed a complete individual spherical form. This result is similar to previous works [31, 32], which showed that hydrocarbons generated from glucose, starch, and cellulose contain an important quantity of micro-spherical particles.

For all the syntesized ACs, their surfaces are richer in microspheres (Fig. 7). This finding may be due to the high applied heat treatment temperature of the hydrochars and the CO_2 activation. Moreover, the AC images show cavities that may be a result of the volatilization of organic matter at 750 °C. These cavities are responsible for the development of micropores and mesopores.

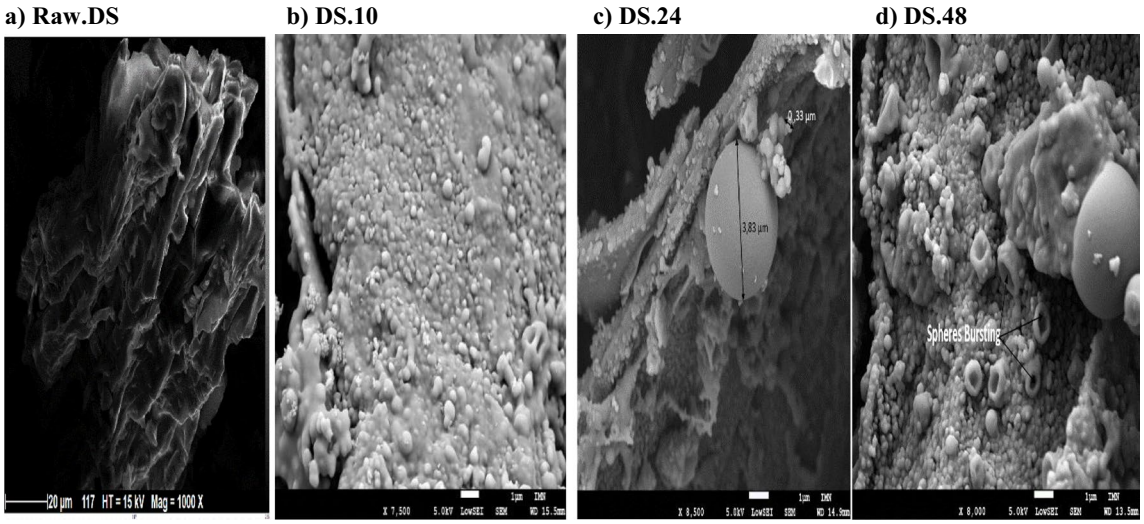

Fig. 5 SEM images of date stone and its derived hydrochars

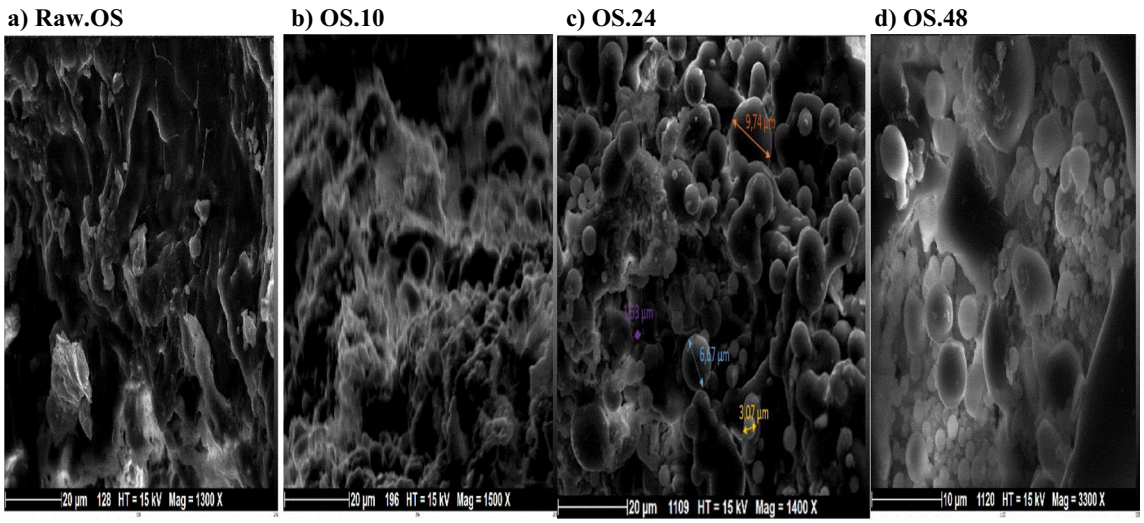

Fig. 6 SEM images of olive stone and its derived hydrochars

3.3 Structural analysis

3.3.1 Raman spectroscopy

Raman spectroscopy has been used for the carbonaceous material characterization [33]. The method of curve-fitting is the easiest technique as it uses only D and G bands [34].

Figure 8 shows the spectra obtained by Raman analyses of hydrochars derived from olive and date stones that are prepared for residence times of 10, 24, and 48 h. The Raman spectra of these three hydrochars show the "D" and "G" bands, as prominent peaks above 1380–1390 cm^{-1} which are associated to the nanocrystalline carbon and the peak at 1585–1610 cm^{-1} that corresponds to amorphous carbon materials (still sp2 bonded), respectively. It is obvious that the "G" band has a higher intensity than the "D" band, indicating the amorphous structure of the materials. Hydrochar of date stones DS-10, DS-24, and DS-48 and olive stones OS-10, OS-24, and OS-48 have I_D/I_G values of 0.70, 0.74, and 0.76 and 0.71, 0.72, and 0.74, respectively.

It is worth mentioning that as the carbonization time increased, the overall Raman intensities decreased. These results may be due to the loss of sensitive groups like oxygenated groups and increasing micro-crystallites (aromatic rings) in the chars [35]. The quantity of aromatic ring systems is growing, which may be linked to the increase in the ID/IG ratios with the increase of the carbonization time. This finding suggests that more carbon defects may exist [33].

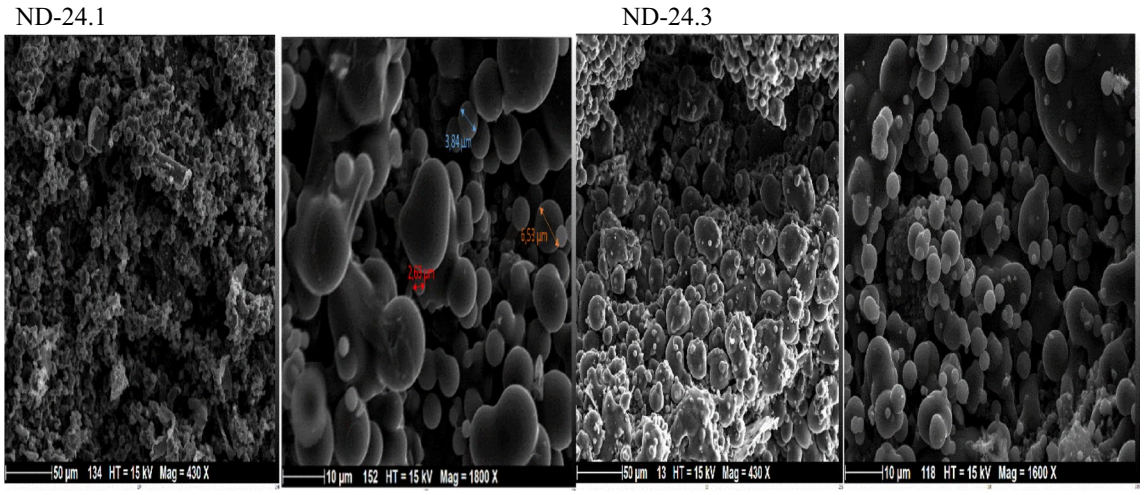

Fig. 7 SEM images of activated carbons

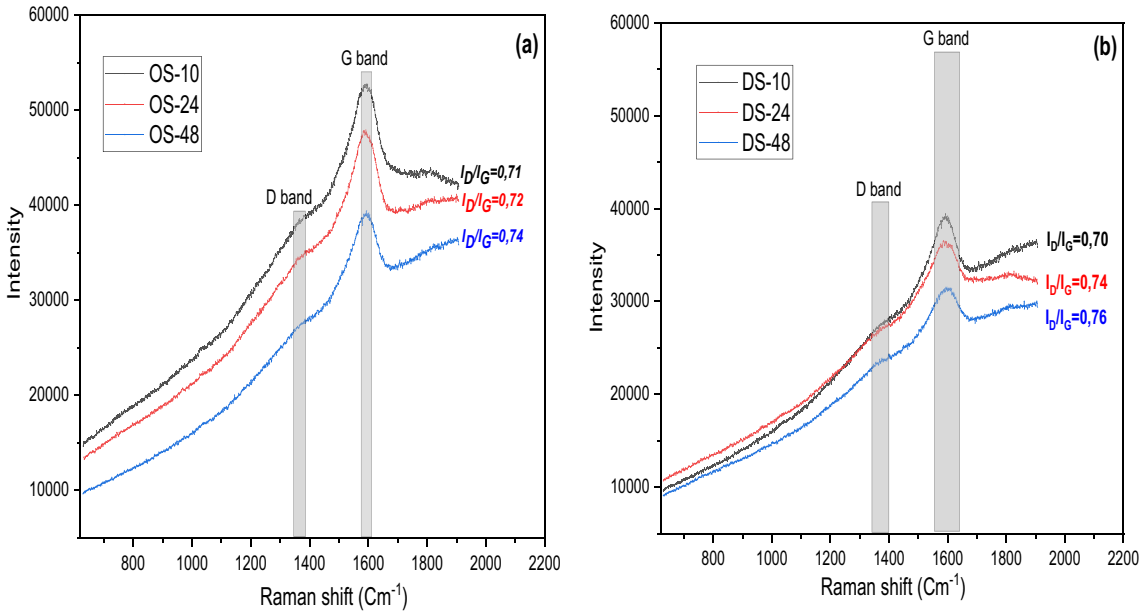

Fig. 8 Raman Spectra analysis of the hydrochars generated from **a** olive and **b** date stones

Furthermore, in the Raman spectra of the activated carbons (Fig. 9), there are two bands located at approximately 1350 and 1600 cm^{-1} representing the structures of amorphous (D-band) and crystalline (G-band) carbon, respectively [33, 36]. The Raman intensities of ACs decreased as compared with the parent hydrochars. This behavior can be explained by the increase in aromaticity of the ACs due to the high activation temperature (750 °C). The peak D changed to a sharp form for the ACs suggesting the increase in their structural order.

3.3.2 X-ray diffraction

Figure 10 gives the XRD spectra of the hydrochar OS-24 and the corresponding activated carbon (OS-24.1). These two spectra have different intensities and exhibit asymmetric peaks corresponding to 2Θ ~25 and 2Θ ~44. The HTC process has removed the microcrystalline structure due to the decomposition of cellulose [37]. A similar finding was reported by Kang S et al. [30] when investigating the hydrothermal carbonization of lignin, cellulose, D-xylose, and wood meal.

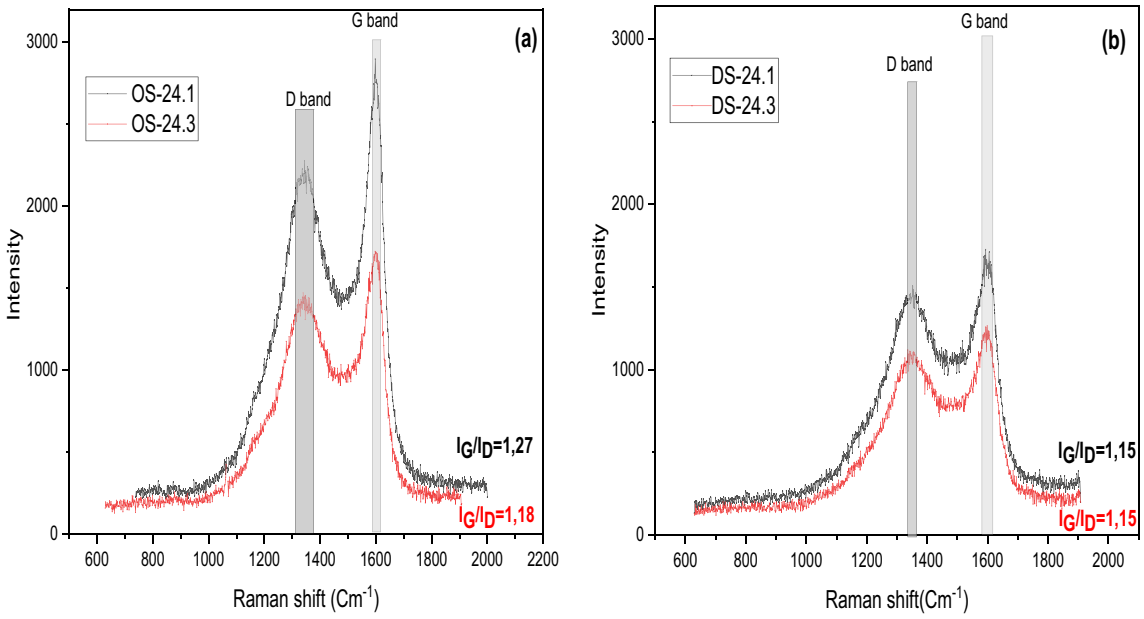

Fig. 9 Spectra of Raman analysis of the synthetized activated carbons from **a** olive stones and **b** date stones

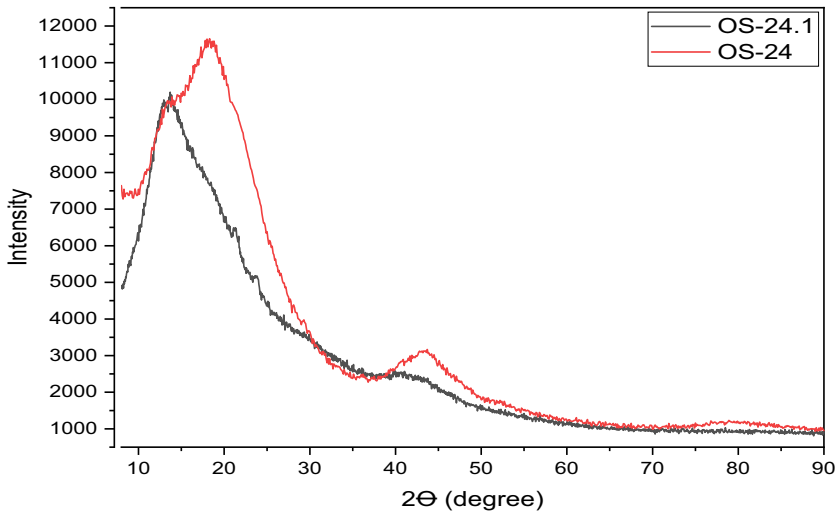

Fig. 10 Diffractogram curve of the hydrochar and activated carbon issued from olive stones

3.4 Functional groups analysis of fruits stones, hydrochars, and activated hydrochars

The functional groups on the surface of biomasses (olive and date stones) and hydrochars are shown in Fig. 11a. The surface functional groups of alkene, ester, ketone, hydroxyl, ether, and carboxyl are present in the raw materials and hydrochars. The raw materials show broad absorption bands with a higher intensity as compared to hydrochars. These results are in agreement with those reported in previous works [20, 38, 39] and confirm the presence of lignin, cellulose, and hemicellulose in the raw biomasses.

Due to the biological nature of biomass material, bands were identified in the wavenumber ranges of 3600–2800 cm^{-1} and 800–1800 cm^{-1} [40]. The spectrum obtained from FTIR analysis of all samples shows an absorption band around 3292 cm^{-1} which is attributed to different -OH (hydroxyl) groups' tensile vibration present in carboxylic and hydroxyl groups [41]. The absorption gaps between 2850 and 2918 cm^{-1} mainly result from the C-H stretching vibrations of the aliphatic molecules [28]. The peak at 1747 cm^{-1} corresponds to the vibrations of the C = O bonds (carboxyl group in cellulose) [39]. The spectrum also shows a band at 1625 cm^{-1} that can be imputed to C = C bond stretching vibrations. The samples represent also some peaks around 1450–1420, 1364, and 1313 cm^{-1}, representing respectively: stretching C=N, deformation C-H, CH_2 bending in cellulose and hemicellulose, and stretching

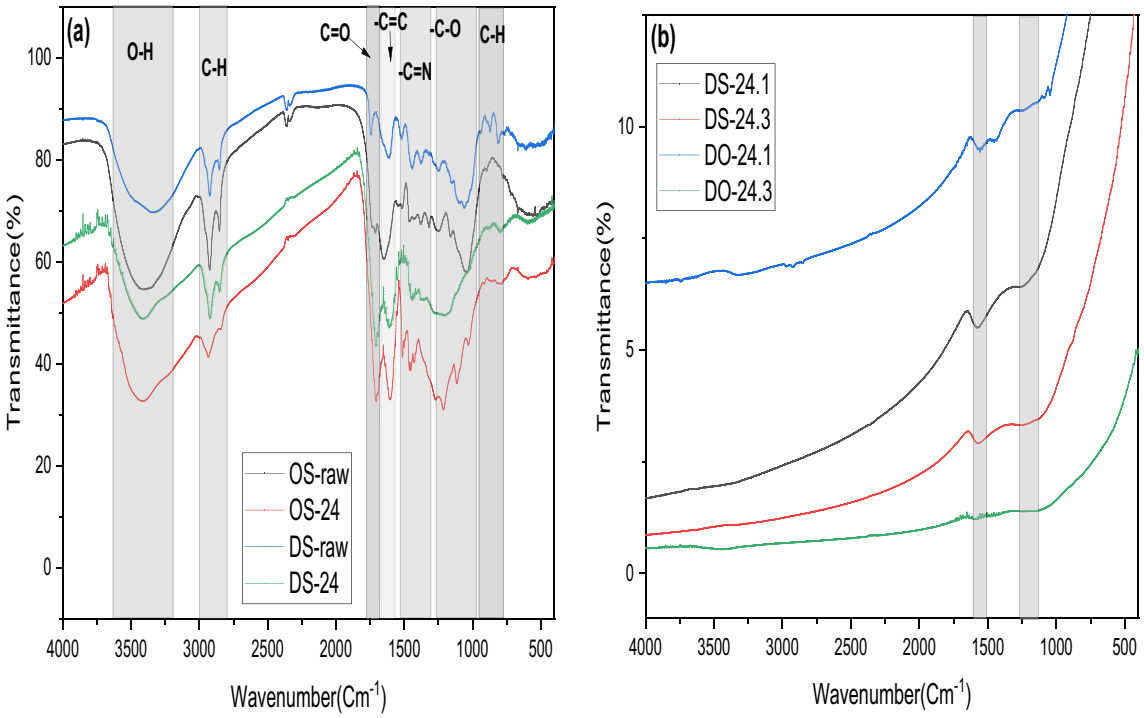

Fig. 11 FTIR analysis of the raw material and its derived hydrochars and activated carbons

–CH_2/-CH_3 of ester [42]. Compressed bands between 927 and 1127 cm^{-1} correspond to C-O bond stretching vibration in cellulose and hemicellulose whereas bands between 1021 and 1099 cm^{-1} are assigned C-O groups in hydrochar samples [38]. Finally, the bands at 810 and 865 cm^{-1} are attributed to the C–H bond out of plane bending of the aromatic ring.

On the other hand, the FTIR spectrum of activated carbons (Fig. 11b) shows that all the bands of the functional groups have disappeared, except the absorption bands between 1000 and 1600 cm^{-1} with a lower intensity than the hydrochar. This behavior may be attributed to the high used activation temperature (750 °C). At this temperature, almost all the surface complexes are eliminated and only the most stable groups are conserved. The spectra of all the ACs exhibit a band at 1600 cm^{-1} that can be attributed to–C = C or –C = O stretching in aldehydes, ketones, or lactones [43]. Additionally, in all the ACs, there is a peak at around 1200 cm^{-1}. This peak can be assigned to the C–OH stretching in phenolic groups.

4 Conclusions

Two series of hydrochars were prepared from date pits and olive stones at 220 °C and residence times of 10, 24, and 48 h. The related generated hydrochars present a high mass yield, an important amount of acidic and basic functional groups, and relatively low porosities. The CO_2 activation of hydrochars for 1 h shows an increase of surface areas from 18 to over 449 $m^2.g^{-1}$ for the date stones and from 20 to over 562 $m^2.g^{-1}$ for the olive stones, with the continuous development of the micro- and meso-pore volumes, and important reduction of both acid and basic functional groups. Hence, it is clearly shown that the CO_2 activation of hydrochars proceeds in the same way as for char activation. Moreover, the increase in the residence time of HTC and the high activation temperature favors the formation of carbon microspheres that lead to significant changes in their surface morphology. Furthermore, the activated carbons prepared from hydrochars show a highly developed spherical structure and present a certain order in structure due to the high activation temperature.

Activated carbons issued from date and olive stone hydrochars present interesting textural and chemical surface characterizations which can be tailored for specific applications such as pollutants removal from aqueous and gaseous effluents, gas storage, supercapacitors, or catalysis.

Acknowledgements The authors gratefully acknowledge the funding organisms.

Author contribution Ahmed Bourafa conceived, carried out the experiments, and wrote the manuscript with support from Meriem Belhachemi. Emna Berrich conceived the sample characterization and contributed to writing the manuscript. Meriem Belhachemi conceived and planned the experiments. Salah Jellali and Mejdi Jeguirim coordinated and contributed to writing the manuscript.

Funding This work was funded by the PHC France—Maghreb (Project No. 20MAG26).

Data availability Not applicable.

Declarations

Ethical approval Not applicable.

Competing interests The authors declare no competing interests.

References

1. Schöpe M (2009) of the European Parliament and of the Council of 23 April 2009 on the promotion of the use of energy from renewable sources and amending and subsequently repealing Directives 2001/77/EC and 2003/30/EC. Eur Wind Energy Conf Exhib 2008 1:32–38. https://data.europa.eu/eli/dir/2009/28/oj
2. Hoang AT, Pham VV, Nguyen XP (2021) Integrating renewable sources into energy system for smart city as a sagacious strategy towards clean and sustainable process. J Clean Prod 305:127161. https://doi.org/10.1016/j.jclepro.2021.127161
3. F A, Ziegler F (2010) Hydrothermal carbonization of biomass: a summary and discussion of chemical mecha- nisms for process engineering Axel. Biofuels Bioprod Biorefining 6:246–256. https://doi.org/10.1002/bbb
4. Belhachemi M (2021) Adsorption of organic compounds on activated carbons. In: Delgado AN (ed) Sorbents Mater Control Environ Pollut Curr State Trends 355–385. https://doi.org/10.1016/B978-0-12-820042-1.00006-7
5. Jain A, Balasubramanian R, Srinivasan MP (2016) Hydrothermal conversion of biomass waste to activated carbon with high porosity: a review. Chem Eng J 283:789–805. https://doi.org/10.1016/j.cej.2015.08.014
6. Thabit Q, Nassour A, Nelles M (2022) Facts and figures on aspects of waste management in Middle East and North Africa Region. Waste 1:52–80. https://doi.org/10.3390/waste1010005
7. Office National des Statistiques (2019) Collection n ° 225 Les Statistiques de l' Agriculture les Productions Vegetales et Animales Rétrospective 2010–2019. https://www.ons.dz/IMG/pdf/retrospective_agricultures2010_2019
8. Stemann J, Erlach B, Ziegler F (2013) Hydrothermal carbonisation of empty palm oil fruit bunches: laboratory trials, plant simulation, carbon avoidance, and economic feasibility. Waste Biomass Valorization 4:441–454. https://doi.org/10.1007/s12649-012-9190-y
9. Zhang S, Zhu X, Zhou S (2018) Hydrothermal carbonization for hydrochar production and its application. In: Yong SO, Tsang DCW, Bolan N, Novak JM (eds) Biochar from Biomass and Waste, pp 275–294. https://doi.org/10.1016/B978-0-12-811729-3.00015-7
10. Kambo HS, Dutta A (2015) A comparative review of biochar and hydrochar in terms of production, physico-chemical properties and applications. Renew Sustain Energy Rev 45:359–378. https://doi.org/10.1016/j.rser.2015.01.050
11. Chen Y, Ai X, Huang B et al (2017) Consecutive preparation of hydrochar catalyst functionalized in situ with sulfonic groups for efficient cellulose hydrolysis. Cellulose 24:2743–2752. https://doi.org/10.1007/s10570-017-1306-x
12. Zhang X, Zhang L, Li A (2017) Hydrothermal co-carbonization of sewage sludge and pinewood sawdust for nutrient-rich hydrochar production: synergistic effects and products characterization. J Environ Manage 201:52–62. https://doi.org/10.1016/j.jenvman.2017.06.018
13. Masoumi S, Borugadda VB, Nanda S et al (2021) Hydrochar a review on its production technologies and applications. Catalysts 11:939–958. https://doi.org/10.3390/catal11080939
14. Belhachemi M, Rios RVRA, Addoun F et al (2009) Preparation of activated carbon from date pits: effect of the activation agent and liquid phase oxidation. J Anal Appl Pyrolysis 86:168–172. https://doi.org/10.1016/j.jaap.2009.05.004
15. Belala Z, Belhachemi M, Jeguirim M (2014) Activated carbon prepared from date pits for the retention of NO2 at low temperature. Int J Chem React Eng 12:717–726. https://doi.org/10.1515/ijcre-2014-0043
16. Prauchner MJ, Rodríguez-Reinoso F (2012) Chemical versus physical activation of coconut shell: a comparative study. Microporous Mesoporous Mater 152:163–171. https://doi.org/10.1016/J.MICROMESO.2011.11.040
17. Román S, Valente Nabais JM, Ledesma B et al (2013) Production of low-cost adsorbents with tunable surface chemistry by conjunction of hydrothermal carbonization and activation processes. Microporous Mesoporous Mater 165:127–133. https://doi.org/10.1016/J.MICROMESO.2012.08.006
18. Yu X, Liu S, Lin G et al (2020) KOH-activated hydrochar with engineered porosity as sustainable adsorbent for volatile organic compounds. Colloids Surf A Physicochem Eng Asp 588:124372. https://doi.org/10.1016/J.COLSURFA.2019.124372
19. Lin Y, Xu H, Gao Y, Zhang X (2021) Preparation and characterization of hydrochar-derived activated carbon from glucose by hydrothermal carbonization. Biomass Convers Biorefinery. https://doi.org/10.1007/s13399-021-01407-y
20. Bouchelta C, Salah M, Bertrand O, Bellat J (2008) Preparation and characterization of activated carbon from date stones by physical activation with steam. J Anal Appl Pyrolysis 82:70–77. https://doi.org/10.1016/j.jaap.2007.12.009
21. Silvestre-Albero J, Gómez de Salazar C, Sepúlveda-Escribano A, Rodríguez-Reinoso F (2001) Characterization of microporous solids by immersion calorimetry. Colloids Surf A Physicochem Eng Asp 187:151–165. https://doi.org/10.1016/S0927-7757(01)00620-3
22. Pari G, Darmawan S, Prihandoko B (2014) Porous carbon spheres from hydrothermal carbonization and KOH activation on cassava and tapioca flour raw material. Procedia Environ Sci 20:342–351. https://doi.org/10.1016/j.proenv.2014.03.043
23. Smith AM, Singh S, Ross AB (2016) Fate of inorganic material during hydrothermal carbonisation of biomass: influence of feedstock on combustion behaviour of hydrochar. Fuel 169:135–145. https://doi.org/10.1016/j.fuel.2015.12.006
24. Missaoui A, Bostyn S, Belandria V et al (2017) Hydrothermal carbonization of dried olive pomace: energy potential and process performances. J Anal Appl Pyrolysis 128:281–290. https://doi.org/10.1016/j.jaap.2017.09.022
25. Hoekman SK, Broch A, Robbins C (2011) Hydrothermal carbonization (HTC) of lignocellulosic biomass. Energy Fuels 25:1802–1810. https://doi.org/10.1021/ef101745n
26. Fernandez ME, Ledesma B, Román S et al (2015) Development and characterization of activated hydrochars from orange peels as potential adsorbents for emerging organic contaminants. Bioresour Technol 183:221–228. https://doi.org/10.1016/j.biortech.2015.02.035
27. Khoshbouy R, Takahashi F, Yoshikawa K (2019) Preparation of high surface area sludge-based activated hydrochar via hydrothermal carbonization and application in the removal of basic dye. Environ Res 175:457–467. https://doi.org/10.1016/j.envres.2019.04.002
28. Zbair M, Bottlinger M, Ainassaari K et al (2020) Hydrothermal carbonization of argan nut shell: functional mesoporous carbon with excellent performance in the adsorption of bisphenol A and diuron. Waste Biomass Valorization 11:1565–1584. https://doi.org/10.1007/s12649-018-00554-0

29. Román S, Nabais JMV, Ledesma B et al (2013) Production of low-cost adsorbents with tunable surface chemistry by conjunction of hydrothermal carbonization and activation processes. Microporous and Mesoporous Materials 165:127–133. https://doi.org/10.1016/j.micromeso.2012.08.006
30. Kang S, Li X, Fan J, Chang J (2012) Characterization of hydrochars produced by hydrothermal carbonization of lignin, cellulose, D-xylose, and wood meal. Ind Eng Chem Res 51:9023–9031. https://doi.org/10.1021/ie300565d
31. Sevilla M, Fuertes AB (2009) Chemical and structural properties of carbonaceous products obtained by hydrothermal carbonization of saccharides. Chem - A Eur J 15:4195–4203. https://doi.org/10.1002/chem.200802097
32. Sevilla M, Maciá-Agulló JA, Fuertes AB (2011) Hydrothermal carbonization of biomass as a route for the sequestration of CO2: chemical and structural properties of the carbonized products. Biomass Bioenerg 35:3152–3159. https://doi.org/10.1016/j.biombioe.2011.04.032
33. Yu J, Sun L, Berrueco C et al (2018) Influence of temperature and particle size on structural characteristics of chars from Beechwood pyrolysis. J Anal Appl Pyrolysis 130:249–255. https://doi.org/10.1016/j.jaap.2018.01.018
34. Xu J, Liu J, Zhang X et al (2020) Chemical imaging of coal in micro-scale with Raman mapping technology. Fuel 264:116826. https://doi.org/10.1016/j.fuel.2019.116826
35. Asadullah M, Zhang S, Min Z et al (2010) Effects of biomass char structure on its gasification reactivity. Bioresour Technol 101:7935–7943. https://doi.org/10.1016/J.BIORTECH.2010.05.048
36. Xu J, Liu J, Ling P et al (2020) Raman spectroscopy of biochar from the pyrolysis of three typical Chinese biomasses: a novel method for rapidly evaluating the biochar property. Energy 202:117644. https://doi.org/10.1016/j.energy.2020.117644
37. Zhang L, Liu S, Wang B (2015) Effect of residence time on hydrothermal carbonization of corn cob residual. BioRes 10:3979–3986. https://doi.org/10.15376/biores.10.3.3979-3986
38. Ralf G, Leahy JJ, Timko MT (2020) Hydrothermal carbonization of olive wastes to produce renewable, binder-free pellets for use as metallurgical reducing agents. Prepr Submitt to Renew Energy
39. Ahmad S, Zhu X, Wei X, Zhang S (2020) Characterization and potential applications of hydrochars derived from P-and N-enriched agricultural and antibiotic residues via microwave-assisted hydrothermal conversion. Energy Fuels 34:11154–11164. https://doi.org/10.1021/acs.energyfuels.0c02149
40. Rizzi V, Agostino FD, Fini P et al (2017) An interesting environmental friendly cleanup: the excellent potential of olive pomace for disperse blue adsorption/desorption from wastewate. Dye Pigment. https://doi.org/10.1016/j.dyepig.2017.01.069
41. Belhachemi M, Khiari B, Jeguirim M, Sepúlveda-Escribano A (2019) Characterization of biomass-derived chars. In Jeguirim M, Limousy L (eds) Char Carbon Mater Deriv from Biomass Prod Charact Appl, pp 69–108. https://doi.org/10.1016/B978-0-12-814893-8.00003-1
42. Azzaz AA, Jeguirim M, Ghimbeu C et al (2019) Olive oil by-products: from harmful waste to interesting carbonaceous materials: hydrothermal conversion of olive oil by-products into carbon rich chars. 2019 10th Int Renew Energy Congr IREC 2019 9:8–12
43. Shi Q, Zhang J, Zhang C et al (2010) Preparation of activated carbon from cattail and its application for dyes removal. J Environ Sci 22:91–97. https://doi.org/10.1016/S1001-0742(09)60079-6